IEEE Access
Multidisciplinary ⋮ Rapid Review ⋮ Open Access Journal

Received March 20, 2019, accepted April 2, 2019, date of publication April 16, 2019, date of current version April 29, 2019.

Digital Object Identifier 10.1109/ACCESS.2019.2911533

Improved Adaptive Hybrid Compensation for Compound Faults of Non-Gaussian Stochastic Systems

KAIYU HU[1], CHANGYUN WEN[2], (Fellow, IEEE), AND AILI YUSUP[3]
[1]College of Automation Engineering, Nanjing University of Aeronautics and Astronautics, Nanjing 211106, China
[2]School of Electrical and Electronic Engineering, NanyangTechnological University, Singapore 639798
[3]National Astronomical Observatory, Chinese Academy of Sciences, Beijing 100101, China

Corresponding author: Kaiyu Hu (hukaiyuluran@126.com)

This work was supported in part by the National Natural Science Foundation of China under Grant 61533009, and in part by the National Basic Research Program (973 Program) under Grant 2015CB857100.

ABSTRACT This study investigates an adaptive estimation and hybrid parallel distribution compensation for non-Gaussian stochastic systems with actuator-sensor compound faults. Type-II fuzzy theory approximates nonlinear dynamical systems with non-Gaussian stochastic outputs and inconsistent response under harsh environments. An estimation observer using fuzzy and improved adaptive laws is proposed to accurately estimate different amplitudes of an actuator fault. In a fault-tolerant controller, the indirect passive compensation factors shield the sensor from the initial fault; therefore, the controller actively compensates for the actuator fault using the estimated information. The output probability density functions then match the expected values. Finally, the Lyapunov functions prove the robust stability and the simulation results indicate the effectiveness of these hybrid methods.

INDEX TERMS Non-Gaussian stochastic systems, nonlinear dynamical systems, compound faults, adaptive estimation, fault-tolerant control, robust stability.

I. INTRODUCTION

Fault diagnosis (FD) and fault-tolerant control (FTC) for complex faults in complex environments can significantly improve system reliability, thereby improving the applicability of the related technologies [1]–[4]. We are committed to studying these key technologies considering compound faults including actuator and sensor faults, system singularity, external disturbance, and output non-Gaussian uncertainty due to harsh environments.

There has been visible progress in the research on FD and FTC of multiple fault types, particularly compound faults. In [5], the problem of diagnosing compound faults over time was solved using a coupled factorial hidden Markov model-based framework. In [6], a frequency blind deconvolution algorithm based on an adaptive generalized morphological filter was proposed for extracting useful signals from the signals contaminated by the compound faults. In [7], the nonlinear FTC and sensor multiple FD for longitudinal dynamics of hypersonic vehicles were designed. In [8], a composite-loop for the FTC under the compound faults was subsequently developed, where newly developed multivariable integral sliding-mode control was integrated. In [9], an improved fast spectral kurtosis method combined with the variational mode decomposition was proposed to improve the tracking accuracy for the compound fault. In [10], an exponentially weighted moving average control chart was constructed to diagnose the compound faults at an early stage. In [11], a low-complexity state feedback FTC scheme that guarantees the prescribed performance was designed for the actuator and component compound faults. In [12], an FTC scheme with higher-order sliding mode-based observers was proposed to provide a continuous drive operation, regardless of any sensor faults. In [13], the robust adaptive FTC addressed the tracking control problem with the prescribed performance to guarantee a rigid system subject to unknown inertia properties, disturbances, actuator faults, and saturation nonlinearities. In [14]–[16], the actuator and sensor compound faults were considered simultaneously when designing controllers, and a similar approach was applied to the system with multiple complex conditions. Even if there is no fault, the parameter errors, singularity, and disturbances should

The associate editor coordinating the review of this manuscript and approving it for publication was Sing Kiong Nguang.

be considered in the harsh environment. In [17], based on the singular approach, the coupled model with parameter errors was decomposed, and a nonlinear hybrid controller was proposed for trajectory tracking and vibration suppression. In [18], a robust sliding mode controller was designed for stabilization of uncertain singular systems with input delay and parameter deviation. In [19], two linear clearance criteria based on structural singular value theory were proposed for the control law. In [20], the cooperative output regulation problem was studied for singular multi-agent systems subject to connected switching networks. In [21]–[23], the inevitable disturbances in the nonlinear systems were considered and the robust controllers were designed to solve the problems of tracking control, FD, and FTC.

Output probability density functions (PDFs) of a non-Gaussian stochastic model can display the distribution information of inaccurate outputs, thereby showing the output distribution laws that regular signals cannot exhibit [24]. By tracing the ideal PDF shapes, the stochastic models can achieve more accurate FTC than the classical models. In [25], a square-root-based algorithm was presented to approximate the output PDF in order to guarantee that PDF was positive. In [26], the Takagi-Sugeno (T-S) theory linearized non-Gaussian nonlinear stochastic systems and a sliding-mode tolerant algorithm compensated for the fault impact on the output PDF. In [27], a reconfigured tolerant controller generated the output when the post-fault stochastic distribution systems had minimum entropy. In [28], a robust, adaptive observer-based FD method was proposed for non-Gaussian uncertain stochastic distribution systems based on the linear B-spline. In [29], an effective FTC strategy with an adaptive distribution compensation control law was proposed in the non-Gaussian systems. This study will use similar compensation methods.

The main contributions of this work can be summarized as follows:

1) Constructing the multi-input multi-output (MIMO) Type II fuzzy non-Gaussian stochastic systems with the singularity and disturbance.

2) Designing an improved adaptive estimation algorithm by integrating actuator fault and fuzzy precondition variable information, which is consistent with the animal predation behavior.

3) Designing the active-passive hybrid FTC for the compound faults: active repair the estimated actuator faults with simultaneously shield the sensor fault without acquiring its information.

A non-Gaussian nonlinear singular stochastic model with external disturbance and compound faults is established using Type-II fuzzy theory in Section II. In Section III, an improved adaptive estimation observer is designed for the actuator fault and the robust stability is proved. In Section IV, an adaptive parallel distribution compensation (PDC) FTC is designed and the robust stability is proved. The novel features of adaptive estimation and FTC in Sections III and IV, namely, fuzzy-prey fusion adaptive strategies, are clarified. In Section V, a three-input three-output non-Gaussian stochastic system that can describe an aeroengine or a stochastic attitude vehicle is employed as the controlled object, and the effectiveness of the FTC under the different fault amplitudes are examined.

II. MODEL

Using the Type-II fuzzy method and considering the singularity, the state equations and weight output equations of non-Gaussian stochastic systems with actuator faults are established as

Rule i: if $f_1(x_1(t))$ is ξ_{i1} is $\ldots f_s(x_s(t))$ is ξ_{is}, THEN

$$\begin{aligned} E\dot{x}(t) &= A_i x(t) + B_i u(t) + H_i F_{tvs}(t) + J_i d(t) \\ V(t) &= D_i x(t) \end{aligned} \tag{1}$$

where: $\xi_{ij}(i = 1, 2, \ldots, p; j = 1, 2, \ldots, s)$ is interval type II fuzzy set, $x(t) \in R^{n\times 1}$ is the state vector, $u(t) \in R^{m\times 1}$ is the control input vector,$F_{tvs}(t) \in R^{m\times 1}$ is the actuator fault vector, $V(t) \in R^{n-1\times 1}$ is the weight vector obtained by multiplying the dimensionality reduction matrix and the state vector, and $d(t) \in R^{m\times 1}$ is the cascade deviation disturbance. $A_i \in R^{n\times n}$, $B_i \in R^{n\times m}$, $H_i \in R^{n\times m}$, $J_i \in R^{n\times m}$ and $D_i \in R^{n-1\times n}$ are the parameter matrices, where D_i is a dimensionality reduction matrix, $E \in R^{n\times n}$ is the singular matrix and satisfies $rank(E) = r < n$. The triggering strength of each fuzzy rule can be expressed as

$$\omega_i(x(t)) = [\omega_{i,low}(x(t)), \omega_{i,up}(x(t))] \tag{2}$$

$$\omega_{i,up}(x(t)) = \prod_{j=1}^{s} \mu_{\xi_{ij},up}(x_j(t)) \tag{3}$$

$$\omega_{i,low}(x(t)) = \prod_{j=1}^{s} \mu_{\xi_{ij},low}(x_j(t)) \tag{4}$$

where $\omega_{i,up}(x(t)) \geq \omega_{i,low}(x(t)) \geq 0$. $\omega_{i,up}(x(t))$ represents the upper membership, and $\omega_{i,low}(x(t))$ is the lower membership. The upper and lower membership functions are represented by $\mu_{\xi_{ij},up}(x_j(t))$ and $\mu_{\xi_{ij},low}(x_j(t))$, respectively. The global Type-II fuzzy model of non-Gaussian stochastic systems with actuator and sensor initial faults can be expressed as

$$\begin{aligned} E\dot{x}(t) &= \sum_{i=1}^{p} (\varphi_{i,low} + \varphi_{i,up})[A_i x(t) + B_i u(t) \\ &\quad + H_i F_{tvs}(t) + J_i d(t)] \end{aligned} \tag{5}$$

$$\begin{aligned} V(t) &= \sum_{i=1}^{p} (\varphi_{i,low} + \varphi_{i,up}) D_i x(t) \\ \gamma(\rho + c, u(t)) &= C(\rho + c)V(t) + T(\rho + c) \end{aligned} \tag{6}$$

where

$$\begin{aligned} \varphi_{i,low} &= \varphi_{i,low}(x(t)) \\ &= \frac{\nu_i(x(t))\omega_{i,low}(x(t))}{\sum_{i=1}^{p} (\nu_i(x(t))\omega_{i,low}(x(t)) + (1 - \nu_i(x(t)))\omega_{i,up}(x(t)))} \end{aligned} \tag{7}$$

$$\varphi_{i,up} = \varphi_{i,up}(x(t)) = \frac{(1-\nu_i(x(t)))\omega_{i,up}(x(t))}{\sum_{i=1}^{r}(\nu_i(x(t))\omega_{i,low}(x(t)) + (1-\nu_i(x(t)))\omega_{i,up}(x(t)))} \tag{8}$$

where $\nu_i(x(t))$ is the weight coefficient and satisfies $0 \leq \nu_i(x(t)) \leq 1$; (6) is the output PDFs generated by the linear B-spline equations with $C(\rho+c) \in R^{\iota\times n-1}$, $T(\rho+c) \in R^{\iota\times 1}$, and $\gamma(\rho+c, u(t)) \in R^{\iota\times 1}$; $\rho = [\rho_1, \ldots, \rho_l, \ldots, \rho_\iota]^T$ is the output real-time measurement without fault; and $c = [c_1, \ldots, c_l, \ldots, c_\iota]^T$ is the sensor initial fault. $l = 1, 2, \ldots, \iota$, $\iota \in Z^+$, and

$$\rho_c = \rho + c = [\rho_1^c, \ldots, \rho_l^c, \ldots, \rho_\iota^c]^T = [\rho_1 + c_1, \ldots, \rho_l + c_l, \ldots, \rho_\iota + c_\iota]^T \tag{9}$$

$$T(\rho_c) = [\phi_{1n}(\rho_1^c)/b_{1n}, \ldots, \phi_{\iota n}(\rho_\iota^c)/b_{\iota n}] \tag{10}$$

$$C(\rho_c) = \begin{bmatrix} \phi_{11}(\rho_1^c) - \frac{\phi_{1n}(\rho_1^c)b_{11}}{b_{1n}}, \ldots, \phi_{1(n-1)}(\rho_1^c) - \frac{\phi_{1n}(\rho_1^c)b_{1(n-1)}}{b_{1n}} \\ \vdots \\ \phi_{\iota 1}(\rho_\iota^c) - \frac{\phi_{\iota n}(\rho_\iota^c)b_{\iota 1}}{b_{\iota n}}, \ldots, \phi_{\iota(n-1)}(\rho_\iota^c) - \frac{\phi_{\iota n}(\rho_\iota^c)b_{\iota(n-1)}}{b_{\iota n}} \end{bmatrix} \tag{11}$$

$$V(t) = [\omega_1, \omega_2, \ldots, \omega_{n-1}]^T \tag{12}$$

$$\begin{cases} \omega_1 b_{11} + \omega_2 b_{12} + \ldots + \omega_n b_{1n} = 1 \\ \vdots \\ \omega_1 b_{\iota 1} + \omega_2 b_{\iota 2} + \ldots + \omega_n b_{\iota n} = 1 \end{cases} \tag{13}$$

$$b_{l\beta} = \int_a^b \phi_{l\beta}(\rho_l^c)d\rho_l^c \tag{14}$$

where $\phi_{l\beta}(\rho_l^c)$ is the β-th basis function of the l-th output, y_c is the output real-time measurement with the sensor initial fault. The actuator fault is defined as

$$F_{tvs}(t) = \begin{cases} F_\sigma(t), & t \in (t_{\sigma 1}, t_{\sigma 2}] \\ 0, & otherwise \end{cases} \tag{15}$$

$$F_\sigma(t) = \begin{cases} F_{\sigma,inc}(t), & t \in (t_{\sigma 1}, t_{\sigma 3}] \\ F_{\sigma,non-inc}(t), & t \in (t_{\sigma 3}, t_{\sigma 2}] \end{cases} \tag{16}$$

$$\begin{cases} \left\|F_{\sigma,inc}(t)/x(t)\right\|_2 \leq 10\% \\ \left\|F_{\sigma,non-inc}(t)/x(t)\right\|_2 > 10\% \end{cases} \tag{17}$$

where $F_{tvs}(t)$ is the intermittent fault with step-varying characteristics, $F_\sigma(t)$ is the value in the fault time interval, $F_{\sigma,inc}(t)$ is the value in the incipient amplitude interval, and $F_{\sigma,non-inc}(t)$ is the value in the residual amplitude interval. $\sigma = 1, \ldots, \sigma_0$ is the number of fault windows. $\|\cdot\|_2$ is the second-order norm.

$d(t)$ is the mean deviation disturbance defined as

$$d(t) = [d_1(t), \ldots, d_m(t)]^T \tag{18}$$

$$d_g(t) = k_g\|c\|_2 + white(t) \tag{19}$$

where white(t) is the white noise, $g = 1, \ldots, m$ kg is the deviation cascade factor.

Remark 1: The initial sensor fault already exists while being bought. The engineering background of (15)~(17) is the deformation and interference of the internal electromechanical systems, intermittent fluid resistance, and electromagnetic interference of the environment. The long-time fault occurrence windows are mostly caused by the environment, and different environmental factors lead to different amplitudes ($F_{inc}(t)$ and $F_{non-inc}(t)$).

Assumption 1: The faults and disturbance are bounded, that is $M_1, M_2, M_3 \in R$ satisfy $\|F_{tvs}(t)\|_2 \leq M_1$, $\|c\|_2 \leq M_2$, and $\|d(t)\|_2 \leq M_3$.

Assumption 2: System (5) is regular and pulseless, i.e.

$$\det(sE - \sum_{i=1}^{p}(\varphi_{i,low} + \varphi_{i,up})A_i) \neq 0, \quad \forall t \geq 0 \tag{20}$$

$$rankE = \deg(sE - \sum_{i=1}^{p}(\varphi_{i,low} + \varphi_{i,up})A_i), \quad \forall t \geq 0 \tag{21}$$

The simplified global Type-II fuzzy model can be expressed as

$$\begin{aligned} E\dot{x}(t) &= A(t)x(t) + B(t)u(t) + H(t)F_{tvs}(t) + J(t)d(t) \\ V(t) &= D(t)x(t) \\ \gamma(\rho_c, u(t)) &= C(\rho_c)V(t) + T(\rho_c) \end{aligned} \tag{22}$$

where

$$A(t) = \sum_{i=1}^{p}(\varphi_{i,low} + \varphi_{i,up})A_i,$$

$$B(t) = \sum_{i=1}^{p}(\varphi_{i,low} + \varphi_{i,up})B_i,$$

$$H(t) = \sum_{i=1}^{p}(\varphi_{i,low} + \varphi_{i,up})H_i,$$

$$J(t) = \sum_{i=1}^{p}(\varphi_{i,low} + \varphi_{i,up})J_i,$$

$$D(t) = \sum_{i=1}^{p}(\varphi_{i,low} + \varphi_{i,up})D_i.$$

And $\gamma(\rho_c, u(t))$ satisfies

$$\begin{aligned} \gamma(\rho_c, u(t)) &= (C(\rho) + \bar{C}(\rho, c))V(t) + T(\rho) + \bar{T}(\rho, c) \\ &= C(\rho)V(t) + \bar{C}(\rho, c)V(t) + T(\rho) + \bar{T}(\rho, c) \\ &= \gamma(\rho, u(t)) + \Delta\gamma(\rho_c, u(t)) \end{aligned} \tag{23}$$

where $\gamma(\rho, u(t))$ is the PDFs when the sensor initial fault is not considered, and $\Delta\gamma(\rho_c, u(t))$ are the errors owing to the sensor initial fault. $\gamma(\rho_c, u(t))$ is the actual output PDFs.

III. ACTUATOR FAULT ESTIMATION

Industrial designs show that the initial sensor amplitude is small, and it usually does not require an estimation algorithm. However, if the actuator fault has a large amplitude and complex time-varying characteristics, it is necessary to design an actuator fault estimation strategy. we design a Type-II fuzzy estimation observer as

Rule i: if $f_1(x_1(t))$ is ξ_{i1} is $\ldots f_s(x_s(t))$ is ξ_{is}, THEN

$$\begin{aligned} E\dot{\hat{x}}(t) &= A_i\hat{x}(t) + B_iu(t) + H_i\hat{F}_{tvs}(t) + L_i\varepsilon_{sum}(t) \\ \hat{V}(t) &= D_i\hat{x}(t) \\ \hat{\gamma}(\rho_c, u(t)) &= C(\rho_c)\hat{V}(t) + T(\rho_c) \\ \varepsilon_{sum}(t) &= \int_a^b \sigma_{mag}(\rho_c)(\hat{\gamma}(\rho_c, u(t)) - \gamma(\rho_c, u(t)))d\rho \\ \dot{\hat{F}}_{tvs}(t) &= -prey\{\Gamma_{i1}\}\hat{F}_{tvs}(t) + prey\{\Gamma_{i2}\}\varepsilon_{sum}(t) \end{aligned} \tag{24}$$

where $\hat{x}(t)$ is the state estimation, $\varepsilon_{sum}(t)$ is the residual, $\hat{F}_{tvs}(t)$ is the actuator fault estimation, L_i is the observer gain matrix, $prey\ \{\Gamma_{i1}\}$ and $prey\ \{\Gamma_{i2}\}$ are the estimation learning rates consistent with the improved predation strategy and are determined by Theorem 1. $\sigma_{mag}(\cdot)$ is a linear magnification function that provides an accurate feedback signal to the observer. $\varepsilon_{sum}(t)$ satisfies

$$\varepsilon_{sum}(t) = \varepsilon(t) + \Delta\varepsilon(t) \tag{25}$$

$$\varepsilon(t) = \int_a^b \sigma_{mag}(\rho)(\hat{\gamma}(\rho, u(t)) - \gamma(\rho, u(t)))d\rho \tag{26}$$

$$\begin{aligned} \Delta\varepsilon(t) = \int_a^b &\sigma_{mag}(\rho)(\Delta\hat{\gamma}(\rho + c, u(t)) - \Delta\gamma(\rho + c, u(t))) \\ &+ \sigma_{mag}(c)(\hat{\gamma}(\rho, u(t)) - \gamma(\rho, u(t)) \\ &+ \Delta\hat{\gamma}(\rho + c, u(t)) - \Delta\gamma(\rho + c, u(t)))d\rho \end{aligned} \tag{27}$$

where $\varepsilon(t)$ and $\Delta\varepsilon(t)$ cannot be separated directly. $\varepsilon(t)$ represents the residual without the measurement errors. Let

$$e_x(t) = \hat{x}(t) - x(t) \tag{28}$$

$$e_{tvs}(t) = \hat{F}_{tvs}(t) - F_{tvs}(t) \tag{29}$$

According to equations (22) and (28), the observation error system is obtained as

$$\begin{aligned} E\dot{e}_x(t) &= \sum_{i=1}^{p}(\varphi_{i,low} + \varphi_{i,up})[A_ie_x(t) + H_ie_{tvs}(t) \\ &\quad + L_i(\Sigma + \Delta\Sigma)D_ie_x(t) - J_id(t)] \\ &= \sum_{i=1}^{p}(\varphi_{i,low} + \varphi_{i,up})\{[A_i + L_i(\Sigma + \Delta\Sigma)D_i]e_x(t) \\ &\quad + H_ie_{tvs}(t) - J_id(t)\} \\ &= \sum_{i=1}^{p}(\varphi_{i,low} + \varphi_{i,up})\{[A_i + L_i\Sigma D_i + L_i\Delta\Sigma D_i]e_x(t) \\ &\quad + H_ie_{tvs}(t) - J_id(t)\} \end{aligned} \tag{30}$$

where

$$\begin{aligned} \Sigma + \Delta\Sigma &= \int_a^b \sigma_{mag}(\rho + c)C(\rho + c)d\rho \\ &= \int_a^b (\sigma_{mag}(\rho) + \sigma_{mag}(c))C(\rho + c)d\rho \\ &= \int_a^b (\sigma_{mag}(\rho)C(\rho + c) + \sigma_{mag}(c)C(\rho + c))d\rho \\ &= \int_a^b \sigma_{mag}(\rho)C(\rho)d\rho + \int_a^b (\sigma_{mag}(\rho)\bar{C}(\rho, c) \\ &\quad + \sigma_{mag}(c)C(\rho) + \sigma_{mag}(c)\bar{C}(\rho, c))d\rho \end{aligned} \tag{31}$$

$$\Sigma = \int_a^b \sigma_{mag}(\rho)C(\rho)d\rho \tag{32}$$

$$\begin{aligned} \Delta\Sigma = \int_a^b &(\sigma_{mag}(\rho)\bar{C}(\rho, c) \\ &+ \sigma_{mag}(c)C(\rho) + \sigma_{mag}(c)\bar{C}(\rho, c))d\rho \end{aligned} \tag{33}$$

Σ is the basis function integral matrix when the sensor initial fault is not considered.

Similarly, the estimation error equation is obtained as

$$\begin{aligned} \dot{e}_{tvs}(t) &= \dot{\hat{F}}_{tvs}(t) - \dot{F}_{tvs}(t) \\ &= \sum_{i=1}^{p}(\varphi_{i,low} + \varphi_{i,up})[-prey\{\Gamma_{i1}\}(e_{tvs}(t) + F_{tvs}(t)) \\ &\quad + prey\{\Gamma_{i2}\}(\Sigma + \Delta\Sigma)D_ie_x(t)] \\ &= \sum_{i=1}^{p}(\varphi_{i,low} + \varphi_{i,up})[-prey\{\Gamma_{i1}\}e_{tvs}(t) \\ &\quad + prey\{\Gamma_{i2}\}(\Sigma + \Delta\Sigma)D_ie_x(t) - prey\{\Gamma_{i1}\}F_{tvs}(t)] \end{aligned} \tag{34}$$

Definition 1: The reference control input is defined as

$$m_1(t) = \sum_{i=1}^{p}(\varphi_{i,low} + \varphi_{i,up})[C_{i1}e_x(t) + C_{i2}e_{tvs}(t)] \tag{35}$$

Theorem 1: When the proper dimension parameters C_{i1}, C_{i2}, R_i, $prey\{\Gamma_{i1}\}$, $prey\{\Gamma_{i2}\}$, and $\lambda_\mu > 0(\mu = 1, 2)$ are determined, there exists a symmetric matrix P for all $i = 1, \ldots, q$ that satisfies

$$E^TP = P^TE \geq 0 \tag{36}$$

$$\begin{bmatrix} \theta_{11} & \theta_{12} & 0 & -P^TJ_i & C_{i1}^T \\ * & -2prey\{\Gamma_{i1}\} & -prey\{\Gamma_{i1}\} & 0 & C_{i2}^T \\ * & * & -\lambda_1^2I & 0 & 0 \\ * & * & * & -\lambda_2^2I & 0 \\ * & * & * & * & -I \end{bmatrix} < 0 \tag{37}$$

and the fuzzy observer gain is $L_i = P^TR_i$, then error observation system (30) is robust stable and satisfies

$$\|m_1(t)\|_2^2 < \lambda_1^2\,\|F_{tvs}(t)\|_2^2 + \lambda_2^2\,\|d(t)\|_2^2 \tag{38}$$

where θ_{11} and θ_{12} are given by

$$\begin{aligned} \theta_{11} = \sum_{i=1}^{p}&(\varphi_{i,low} + \varphi_{i,up})(A_iP + P^TA_i + D_i^T\Sigma^TR_i^T \\ &+ D_i^T\Delta\Sigma^TR_i^T + R_i\Sigma D_i + R_i\Delta\Sigma D_i) \end{aligned} \tag{39}$$

$$\theta_{12} = \sum_{i=1}^{p}(\varphi_{i,low}+\varphi_{i,up})(P^T H_i + D_i^T \Sigma^T prey\{\Gamma_{i2}^T\} + D_i^T \Delta\Sigma^T prey\{\Gamma_{i2}^T\}) \quad (40)$$

Proof: Select the Lyapunov function candidate as

$$V_1(t) = e_x^T(t)E^T P e_x(t) + e_{tvs}^T(t)e_{tvs}(t) \quad (41)$$

Assume $V_1(0)=0$ and combine (30)(34), the first derivative of $V_1(t)$ can be expressed as

$$\begin{aligned}
&\dot{V}_1(t) \\
&= \dot{e}_x^T(t)E^T P e_x(t) + e_x^T(t)E^T P\dot{e}_x(t) + 2e_{tvs}^T(t)\dot{e}_{tvs}(t) \\
&= \sum_{i=1}^{p}(\varphi_{i,low}+\varphi_{i,up})\{[(A_i + L_i(\Sigma+\Delta\Sigma)D_i)e_x(t) \\
&\quad + H_i e_{tvs}(t) - J_i d(t)]^T P e_x(t) + e_x^T(t)P^T[(A_i + L_i(\Sigma \\
&\quad + \Delta\Sigma)D_i)e_x(t) + H_i e_{tvs}(t) - J_i d(t)] + 2e_{tvs}^T(t)\dot{e}_{tvs}(t) \\
&= \sum_{i=1}^{p}(\varphi_{i,low}+\varphi_{i,up})\{e_x^T(t)[(A_i + L_i(\Sigma+\Delta\Sigma)D_i)^T P \\
&\quad + P^T(A_i + L_i(\Sigma+\Delta\Sigma)D_i)]e_x(t) + 2e_x^T(t)P^T H_i e_{tvs}(t) \\
&\quad - 2e_x^T(t)P^T J_i d(t) + 2e_{tvs}^T(t)\dot{e}_{tvs}(t)\}
\end{aligned} \quad (42)$$

Substitute (34) to (42), (43) can be derived as

$$\begin{aligned}
&\dot{V}_1(t) \\
&= \sum_{i=1}^{p}(\varphi_{i,low}+\varphi_{i,up})\{e_x^T(t)[(A_i + L_i(\Sigma+\Delta\Sigma)D_i)^T P \\
&\quad + P^T(A_i + L_i(\Sigma+\Delta\Sigma)D_i)]e_x(t) + 2e_x^T(t)P^T H_i e_{tvs}(t) \\
&\quad - 2e_x^T(t)P^T J_i d(t) + 2e_{tvs}^T(t)[-prey\{\Gamma_{i1}\}e_{tvs}(t) \\
&\quad + prey\{\Gamma_{i2}\}(\Sigma+\Delta\Sigma)D_i e_x(t) - prey\{\Gamma_{i1}\}F_{tvs}(t)]\} \\
&= \sum_{i=1}^{p}(\varphi_{i,low}+\varphi_{i,up})\{e_x^T(t)[(A_i + L_i\Sigma D_i + L_i\Delta\Sigma D_i)^T P \\
&\quad + P^T(A_i + L_i\Sigma D_i + L_i\Delta\Sigma D_i)]e_x(t) + 2e_x^T(t)P^T H_i e_{tvs}(t) \\
&\quad - 2e_x^T(t)P^T J_i d(t) - 2e_{tvs}^T(t)prey\{\Gamma_{i1}\}e_{tvs}(t) \\
&\quad + 2e_{tvs}^T(t)prey\{\Gamma_{i2}\}\Sigma D_i e_x(t) \\
&\quad + 2e_{tvs}^T(t)prey\{\Gamma_{i2}\}\Delta\Sigma D_i e_x(t) - 2e_{tvs}^T(t)prey\{\Gamma_{i1}\}F_{tvs}(t)\}
\end{aligned} \quad (43)$$

Based on (43), the robust performance indicator is derived as

$$\begin{aligned}
&\|m_1(t)\|_2^2 - \lambda_1^2\|F_{tvs}(t)\|_2^2 - \lambda_2^2\|d(t)\|_2^2 + \dot{V}_1(t) \\
&= \sum_{i=1}^{p}(\varphi_{i,low}+\varphi_{i,up})\{[C_{i1}e_x(t) + C_{i2}e_{tvs}(t)]^T[C_{i1}e_x(t) \\
&\quad + C_{i2}e_{tvs}(t)]\} - \lambda_1^2 F_{tvs}^T(t)F_{tvs}(t) - \lambda_2^2 d^T(t)d(t) + \dot{V}_1(t) \\
&= \sum_{i=1}^{p}(\varphi_{i,low}+\varphi_{i,up})\{e_x^T(t)C_{i1}^T C_{i1}e_x(t) + e_x^T(t)C_{i1}^T C_{i2}e_{tvs}(t) \\
&\quad + e_{tvs}^T(t)C_{i2}^T C_{i1}e_x(t) + e_{tvs}^T(t)C_{i2}^T C_{i2}e_{tvs}(t)\} \\
&\quad - \lambda_1^2 F_{tvs}^T(t)F_{tvs}(t) - \lambda_2^2 d^T(t)d(t) + \dot{V}_1(t) \\
&= \sum_{i=1}^{p}(\varphi_{i,low}+\varphi_{i,up})q^T(t)\Phi_1 q(t)
\end{aligned} \quad (44)$$

where

$$q^T(t) = [\,e_x^T(t)\ \ e_{tvs}^T(t)\ \ F_{tvs}^T(t)\ \ d^T(t)\,] \quad (45)$$

$$\Phi_1 = \begin{bmatrix} \Lambda_{11}+C_{i1}^T C_{i1} & \Lambda_{12}+C_{i1}^T C_{i2} & 0 & -P^T J_i \\ * & -2prey\{\Gamma_{i1}\}+C_{i2}^T C_{i2} & -prey\{\Gamma_{i1}\} & 0 \\ * & * & -\lambda_1^2 I & 0 \\ * & * & * & -\lambda_2^2 I \end{bmatrix} = \begin{bmatrix} \Lambda_{11} & \Lambda_{12} & 0 & -P^T J_i \\ * & -2prey\{\Gamma_{i1}\} & -prey\{\Gamma_{i1}\} & 0 \\ * & * & -\lambda_1^2 I & 0 \\ * & * & * & -\lambda_2^2 I \end{bmatrix} + C_{i3}^T C_{i3} \quad (46)$$

In (46), C_{i3}, Λ_{11}, and Λ_{12} satisfy

$$C_{i3} = [\,C_{i1}\quad C_{i2}\quad 0\quad 0\,] \quad (47)$$

$$\Lambda_{11} = (A_i + L_i\Sigma D_i + L_i\Delta\Sigma D_i)^T P + P^T(A_i + L_i\Sigma D_i + L_i\Delta\Sigma D_i) \quad (48)$$

$$\Lambda_{12} = P^T H_i + D_i^T\Sigma^T prey\{\Gamma_{i2}^T\} + D_i^T\Delta\Sigma^T prey\{\Gamma_{i2}^T\} \quad (49)$$

Applying the Schur lemma to inequality (37), we obtain $\Phi_1 < 0$. Therefore, the following inequality is obtained:

$$\|m_1(t)\|_2^2 - \lambda_1^2\|F_{tvs}(t)\|_2^2 - \lambda_2^2\|d(t)\|_2^2 + \dot{V}_1(t) < 0 \quad (50)$$

Integrate both sides of inequality (50) over the interval $[0, T]$:

$$\begin{aligned}
&\int_0^T (\|m_1(t)\|_2^2 - \lambda_1^2\|F_{tvs}(t)\|_2^2 - \lambda_2^2\|d(t)\|_2^2 + \dot{V}_1(t))dt \\
&= \int_0^T \|m_1(t)\|_2^2 dt - \int_0^T \lambda_1^2\|F_{tvs}(t)\|_2^2 dt - \int_0^T \lambda_2^2\|d(t)\|_2^2 dt \\
&\quad + V_1(T) - V_1(0) < 0
\end{aligned} \quad (51)$$

When $T \to \infty$ and $V_1(T) \geq 0$, inequality (51) can be expressed as

$$\|m_1(t)\|_2^2 - \lambda_1^2\|F_{tvs}(t)\|_2^2 - \lambda_2^2\|d(t)\|_2^2 - V_1(0) < 0 \quad (52)$$

Therefore, the following conclusion can be obtained:

$$\|m_1(t)\|_2^2 < \lambda_1^2\|F_{tvs}(t)\|_2^2 + \lambda_2^2\|d(t)\|_2^2 \quad (53)$$

Theorem 1 is proved. □

Therefore, the designed observer can effectively estimate actuator faults under the disturbance and sensor initial fault, which create conditions for active FTC.

IV. COMPOUND FTC AND PREY STRATEGY

Based on the characteristics of compound faults with actuator and sensor initial faults, an improved fusion variable parameter compensation algorithm is used to repair the systems.

Remark 2: The expected PDFs are generated by ground tests without considering the sensor initial fault, but to simplify the model, we use uniform basis function matrices and compensate for the impact of this simplification by adjusting the expected weights. The effect of the sensor initial fault on the PDFs using B-spline functions is replaced by the effect of expected weight adjustment on PDFs. The correspondence between the two effects can be obtained through ground tests.

When the B-spline functions are determined, according to Remark 2, the output angle PDF shapes only depend on the weights, so the PDFs tracking is converted into the weights tracking. The expected PDFs are expressed as

$$\gamma_{expe} = C(\rho_c)V_{expe} + T(\rho_c) \tag{54}$$

where V_{expe} is the expected weight vector. The tracking errors of PDFs $E(\rho_c, u(t))$ are defined as

$$\begin{aligned} E(\rho_c, u(t)) &= E_{ftc} = \gamma(\rho_c, u(t)) - \gamma_{expe} \\ &= C(\rho + c)V(t) + T(\rho + c) \\ &\quad - C(\rho + c)V_{expe} - T(\rho + c) \\ &= C(\rho + c)e_v(t) \end{aligned} \tag{55}$$

where $e_v(t) = V(t)$-V_{expe} is the weight error vector. Obviously, if $e_v(t)$ converges to a sufficiently small constant, $E(\rho_c, u(t))$ will have a similar convergence.

When faults exist, the designed controller ensures that systems achieve the performance without fault and the output PDFs accurately track the given distributions. System (22) can be represented as

$$\bar{E}\dot{z}(t)=\sum_{i=1}^{p}(\varphi_{i,low}+\varphi_{i,up})(\bar{A}_i z(t)+\bar{B}_i u(t)+\bar{H}_i F_{tvs}(t)+d_1(t)) \tag{56}$$

where:

$$\bar{E}_i = \begin{bmatrix} E & 0 \\ 0 & I \end{bmatrix}, \quad \bar{A}_i = \begin{bmatrix} A_i & 0 \\ D_i & 0 \end{bmatrix}, \bar{B}_i = \begin{bmatrix} B_i \\ 0 \end{bmatrix},$$
$$\bar{H}_i = \begin{bmatrix} H_i \\ 0 \end{bmatrix}, \quad d_1(t) = \begin{bmatrix} J_i d(t) \\ -V_g \end{bmatrix},$$
$$z(t) = [\, x^T(t) \quad (\textstyle\int_0^t (V(t) - V_{expe})d\tau)^T \,]^T.$$

Assumption 3: A suitable dimension matrix M satisfies $\bar{B}(t)M = \bar{H}(t)$.

The PDC fuzzy-prey adaptive FTC in the fault environment is

$$u_1(t) = \sum_{i=1}^{p}(\varphi_{i,low} + \varphi_{i,up})(prey\{\Omega_i\} + \Gamma_{i3}e_{ftc}\Gamma_{i4})z(t) - MF_{tvs}(t) \tag{57}$$

where: $prey\{\Omega_i\}$ is the gain matrix that obeys the prey adaptive rules, and Γ_{i3} and Γ_{i4} are the compensation factors. e_{ftc}satisfies

$$e_{ftc} = \int_a^b \sigma_{mag}(\rho_c)E_{ftc}d\rho \tag{58}$$

e_{ftc} contains the influence of the sensor initial fault on the tracking errors of the output PDFs. Γ_{i3} and Γ_{i4} are introduced to shield this effect. From the closed-loop dynamic systems (56) and (57), (59) can be obtained as

$$\bar{E}\dot{z}(t) = \sum_{i=1}^{p}(\varphi_{i,low} + \varphi_{i,up})\{(\bar{A}_i + \bar{B}_i prey\{\Omega_i\} + \Gamma_{i3}e_{ftc}\Gamma_{i4})z(t) + \tilde{H}_i d_2(t)\} \tag{59}$$

where $\tilde{H}_i = [\,-\bar{H}_i \; I\,]$, $d_2(t) = [\, e_{tvs}^T(t) \; d_1^T(t)\,]^T$.

Definition 2: The system reference input is defined as

$$m_3(t) = \sum_{i=1}^{p}(\varphi_{i,low} + \varphi_{i,up})C_{i6}z(t) \tag{60}$$

where C_{i6} is a parameter matrix with proper dimensions.

Theorem 2: When $\lambda_4 > 0$, proper dimension matrices C_{i6} and N_{i2} are determined, and there exists a matrix $X_2 > 0$ for all $i = 1, 2, \ldots, q$ that satisfies:

$$X_2\bar{E}^T = \bar{E}X_2^T \geq 0 \tag{61}$$
$$\Xi_{ii} < 0, \quad i = 1, 2, \ldots, q \tag{62}$$
$$\Xi_{ij} + \Xi_{ji} < 0, \quad i < j \leq q \tag{63}$$

Then, the closed-loop system (59) is robust and stable and the robust performance H∞ satisfies

$$\|m_3(t)\|_2 < \sum_{i=1}^{p}(\varphi_{i,low} + \varphi_{i,up})\lambda_4 \|d_2(t)\|_2 \tag{64}$$

where $X_2 = P_2^{-T}$, $N_{i2} = (prey\{\Omega_i\} + \Gamma_{i3}e_{ftc}\Gamma_{i4})X_2^T$, $\Xi_{ij} = \begin{bmatrix} \xi_{11} & \tilde{H}_i & XC_{i4}^T \\ * & -\lambda_3^2 I & 0 \\ * & * & -I \end{bmatrix}$. In Ξ_{ij}:

$$\xi_{11} = X_2\bar{A}_i^T + \bar{A}_i X_2^T + N_{j2}^T\bar{B}_i^T + \bar{B}_i N_{j2} \tag{65}$$

Proof: Select the generalized Lyapunov function candidate as

$$V_2(t) = z^T(t)\bar{E}^T P_2 z(t) \tag{66}$$

Assume $V_2(0) = 0$. Combining (59) and (61), the derivative of $V_2(t)$ can be expressed as

$$\begin{aligned} &\dot{V}_2(t) \\ &= \dot{z}^T(t)\bar{E}^T P_2 z(t) + z^T(t)\bar{E}^T P_2\dot{z}(t) \\ &= \sum_{i=1}^{p}(\varphi_{i,low} + \varphi_{i,up})\{[\bar{A}_i + \bar{B}_i(prey\{\Omega_i\} \\ &\quad + \Gamma_{i3}e_{ftc}\Gamma_{i4})]z(t) + \tilde{H}_i d_2(t)\}^T P_2 z(t) \\ &\quad + \sum_{i=1}^{p}(\varphi_{i,low} + \varphi_{i,up})z^T(t)P_2^T\{[\bar{A}_i \\ &\quad + \bar{B}_i(prey\{\Omega_i\} + \Gamma_{i3}e_{ftc}\Gamma_{i4})]z(t) + \tilde{H}_i d_1(t)\} \\ &= \sum_{i=1}^{p}(\varphi_{i,low} + \varphi_{i,up})z^T(t)\{[\bar{A}_i + \bar{B}_i(prey\{\Omega_i\} \\ &\quad + \Gamma_{i3}e_{ftc}\Gamma_{i4})]^T P_2 + P_2^T[\bar{A}_i + \bar{B}_i(prey\{\Omega_i\} \\ &\quad + \Gamma_{i3}e_{ftc}\Gamma_{i4})]\}z(t) + 2z^T(t)P_2^T\sum_{i=1}^{p}(\varphi_{i,low} + \varphi_{i,up})\tilde{H}_i d_2(t) \end{aligned} \tag{67}$$

When $d_2(t) = 0$, it can be known from (62) and (63) that the following inequality holds

$$\sum_{i=1}^{p}(\varphi_{i,low}+\varphi_{i,up})\{[\bar{A}_i+\bar{B}_i(prey\{\Omega_i\}+\Gamma_{i3}e_{ftc}\Gamma_{i4})]^T P_2 + P_2^T[\bar{A}_i+\bar{B}_i(prey\{\Omega_i\}+\Gamma_{i3}e_{ftc}\Gamma_{i4})]\} < 0 \quad (68)$$

Hence $\dot{V}_2(t) < 0$. So, when $d_2(t) = 0$, the closed-loop system (59) has a large-scale asymptotic stability. If $d_2(t) \neq 0$, (69) is obtained as

$$\begin{aligned}\|m_3(t)\|^2 - \lambda_4^2\|d_2(t)\|^2 + \dot{V}_2(t) &= \sum_{i=1}^{p}(\varphi_{i,low}+\varphi_{i,up})(z^T(t)C_{i6}^T C_{i6}z(t) \\ &\quad - \lambda_4^2 d_2^T(t)d_2(t)) + \dot{V}_2(t) = q_2^T(t)S_2 q_2(t) \end{aligned} \quad (69)$$

where

$$q_2^T(t) = [\,z^T(t) \quad d_2^T(t)\,] \quad (70)$$

$$\begin{aligned} S_2 &= \sum_{i=1}^{p}(\varphi_{i,low}+\varphi_{i,up})(\begin{bmatrix}\bar{S}_{11} & P_2^T\tilde{H}_i \\ * & -\lambda_4^2 I\end{bmatrix} + C_{i7}^T C_{i7}) \\ &= \sum_{i=1}^{p}(\varphi_{i,low}+\varphi_{i,up})\begin{bmatrix}\bar{S}_{11}+C_{i6}^T C_{i6} & P_2^T\tilde{H}_i \\ * & -\lambda_4^2 I\end{bmatrix} \end{aligned} \quad (71)$$

$$C_{i7} = [\,C_{i6} \quad 0\,] \quad (72)$$

$$\bar{S}_{11} = [\bar{A}_i+\bar{B}_i(prey\{\Omega_i\}+\Gamma_{i3}e_{ftc}\Gamma_{i4})]^T P_2 + P_2^T[\bar{A}_i + \bar{B}_i(prey\{\Omega_i\}+\Gamma_{i3}e_{ftc}\Gamma_{i4})] \quad (73)$$

Applying Schur's lemma to inequalities (62) and (63), we obtain: $S_2 < 0$. Hence

$$\|m_3(t)\|_2^2 - \lambda_4^2\|d_2(t)\|_2^2 + \dot{V}_2(t) < 0 \quad (74)$$

Taking integral to both sides of the inequality (74):

$$\begin{aligned}\int_0^T (\|m_3(t)\|_2^2 - \lambda_4^2\|d_2(t)\|_2^2 + \dot{V}_2(t))dt &= \int_0^T \|m_3(t)\|_2^2\,dt - \int_0^T \lambda_4^2\|d_2(t)\|_2^2 dt \\ &\quad + V_2(t) - V_2(0) < 0\end{aligned} \quad (75)$$

Because $T \to \infty \Rightarrow V_2(T) \geq 0$, (75) can be written as

$$\|m_3(t)\|_2^2 - \lambda_4^2\|d_2(t)\|_2^2 - V_2(0) < 0 \quad (76)$$

Finally the following conclusions can be obtained as

$$\|m_3(t)\|_2 < \lambda_4\|d_2(t)\|_2 \quad (77)$$

Theorem 2 is proved. □

Replacing $x(t)$, e_{ftc} and $F_{tvs}(t)$ in (57) with, and we can obtain a practical PDC fuzzy-prey fusion adaptive tolerant controller:

$$u_1(t)\sum_{i=1}^{p}(\varphi_{i,low}+\varphi_{i,up})(prey\{\Omega_i\}+\Gamma_{i3}\hat{e}_{ftc}\Gamma_{i4})\hat{z}(t) - M\hat{F}_{tvs}(t) \quad (78)$$

TABLE 1. Insensitive prey strategy.

Cheetah		*Antelope*	
Distance	*Status*	*Judgment*	*Response*
Far	Progressive	Safe	Static
Close	Progressive	Safe	Static
Close	Run	Threat	Run

TABLE 2. Ftc insensitive prey algorithm.

Fault		*Controller*	
Distance	*Status*	*Judgment*	*Response*
$(0, \kappa]$	Fault free	Small impact	$\Omega_{i1}/\Gamma_{i11}/\Gamma_{i21}$
$(0.1\|\hat{x}(t)\|_2, M_1]$	Fault $F_{\sigma,inc}$	Small impact	$\Omega_{i1}/\Gamma_{i11}/\Gamma_{i21}$
$(\kappa, 0.1\|\hat{x}(t)\|_2]$	Fault $F_{\sigma,non\text{-}inc}$	Big impact	$\Omega_{i2}/\Gamma_{i12}/\Gamma_{i22}$

where

$$\hat{z}(t) = [\hat{x}^T(t)(\int_0^t(\hat{V}(\tau)-V_g)d\tau)^T]^T,$$

$$\hat{e}_{ftc} = \int_a^b(\hat{\gamma}(\rho_c, u(t)) - \gamma_{expe})d\rho,$$

$$\hat{V}(t) = \sum_{i=1}^{p}(\varphi_{i,low}+\varphi_{i,up})D_i(\hat{x}(t)+\Delta\hat{x}(t)).$$

The idea of prey strategy originates from the animal hunting process on the grassland. Taking cheetah/antelope as an example, there are three correspondences in the predation process: cheetah (progressive, far) → antelope (safe, static); cheetah (progressive, close) → antelope (safe, static) or (threat, run); cheetah (run, close) → antelope (threat, run). The antelope can easily and efficiently cope with the complex predation state in two ways. So the prey strategy is a simple adaptive strategy. Replace cheetah with fault, antelope with controller, Table 1 gives the corresponding relationship in the insensitive prey strategy. Where Ω_{i1}, Ω_{i2}, Γ_{i11}, Γ_{i21}, Γ_{i12}, Γ_{i22} are the LMI-compliant adaptive learning rates, is a threshold that is approximately zero.

Remark 3: According to the characteristics of prey strategy, the boundary state of judging threat from cheetah (slow approach, close) corresponds to the boundary state interval in which the controller determines the fault magnitude, as shown in Table 1 and 2. The insensitive prey controller determines that the faults in the interval have little effect and hence do not change the learning rates. The sensitive prey controller is the opposite.

The algorithm steps are as follows:

Step 1: Fault amplitude is less than or equal to κ, no fault, parameters are set to $\Omega_{i1}/\Gamma_{i11}/\Gamma_{i21}$.

Step 2: Fault amplitude is larger than κ and less than or equal to $0.1\,\|\hat{x}(t)\|_2$, incipient fault, parameters are insensitive and set to $\Omega_{i1}/\Gamma_{i11}/\Gamma_{i21}$.

Step 3: Fault amplitude is larger than $0.1\,\|\hat{x}(t)\|_2$, large value fault, parameters are set to $\Omega_{i2}/\Gamma_{i12}/\Gamma_{i22}$.

Step 4: Return to Step 1 without modifying content.

Based on Table 1 and 2, (24) and (57) are improved to the fuzzy-prey fusion adaptive estimation and FTC:

$$\dot{\hat{F}}_{tvs}(t) = \sum_{i=1}^{p} (\varphi_{i,low} + \varphi_{i,up})(-prey\{\Gamma_{i1}\}\hat{F}_{tvs}(t) + prey\{\Gamma_{i2}\}\varepsilon_{sum}(t)) \tag{79}$$

$$u_1(t) = \sum_{i=1}^{p} (\varphi_{i,low} + \varphi_{i,up})(prey\{\Omega_i\} + \Gamma_{i3}\hat{e}_{ftc}\Gamma_{i4})\hat{z}(t) - M\hat{F}_{tvs}(t) \tag{80}$$

where $prey\{\cdot\}$ is the fusion adaptive functions designed according to the fuzzy and prey strategies that satisfy:

$$prey\{\Omega_i, \Gamma_{i1}, \Gamma_{i2}\} = \begin{cases} \Omega_{i1}, \Gamma_{i11}, \Gamma_{i21}, \left\|\hat{F}_{tvs}(t)\right\|_2 \le 0.1 \left\|\hat{x}(t)\right\|_2 \\ \Omega_{i2}, \Gamma_{i12}, \Gamma_{i22}, \left\|\hat{F}_{tvs}(t)\right\|_2 > 0.1 \left\|\hat{x}(t)\right\|_2 \end{cases} \tag{81}$$

V. SIMULATION

The MIMO non-Gaussian stochastic systems can express the control process such as multi-axis vibration control of parallel servo systems, and stochastic attitude aircraft control. Referring to the general hypersonic vehicle attitude models, We select a 3-input 3-output non-Gaussian stochastic system to verify the algorithms presented in this paper. The B-spline functions are set as

$$\begin{cases} \phi_{\beta=1}(\rho_1)=\phi_{\beta=2}(\rho_2)=\phi_{\beta=3}(\rho_3) = Z_1I_1+Z_4I_2+Z_7I_3 \\ \phi_{\beta=2}(\rho_1)=\phi_{\beta=1}(\rho_2)=\phi_{\beta=1}(\rho_3) = Z_2I_2+Z_5I_3+Z_8I_4 \\ \phi_{\beta=3}(\rho_1)=\phi_{\beta=3}(\rho_2)=\phi_{\beta=2}(\rho_3) = Z_3I_3+Z_6I_4+Z_9I_5 \end{cases} \tag{82}$$

where $Z_1 = 0.5(\rho_l + c_l - 2)^2$, $Z_2 = 0.5(\rho_l + c_l - 3)^2$, $Z_3 = 0.5(\rho_l + c_l - 4)^2$, $Z_4 = -(\rho_l + c_l)^2 + 7(\rho_l + c_l) - 11.5$, $Z_5 = -(\rho_l + c_l)^2 + 9(\rho_l + c_l) - 19.5$, $Z_6 = -(\rho_l + c_l)^2 + 11(\rho_l + c_l) - 29.5$, $Z_7 = 0.5(\rho_l + c_l - 5)^2$, $Z_8 = 0.5(\rho_l + c_l - 6)^2$, $Z_9 = 0.5(\rho_l + c_l - 7)^2$, c_l satisfies: $c_l = 0.05$, and I_O satisfies:

$$I_O = \begin{cases} 1 & \rho_l \in [O+1, O+2] \\ 0 & otherwise. \end{cases}$$

where $O = 1, 2, 3, 4, 5$. The ideal initial values are: $x_{initial} = [0.10.10.1]^T$. Referring to system (22) and adding the compound faults with the actuator fault and the sensor fault, the simulation system can be obtained. where the specific values of parameter matrices are as follows:

$$E = \begin{bmatrix} 1 & 0 & 0 \\ 0 & 1 & 0 \\ 0 & 0 & 0 \end{bmatrix}, \quad A_1 = \begin{bmatrix} -1 & 2 & 0 \\ 0 & -2 & 7 \\ 0 & 5 & 6 \end{bmatrix},$$

$$A_2 = \begin{bmatrix} -1 & 1 & 0 \\ 2 & -1 & 0 \\ 0 & 0.6 & 2 \end{bmatrix}, \quad B_1 = \begin{bmatrix} 1 & 1 & -0.01 \\ 0 & 2 & -0.02 \\ 0.002 & 0.005 & 0.1 \end{bmatrix},$$

$$B_2 = \begin{bmatrix} 1.9 & 1.9 & -0.1 \\ 0 & 2 & -0.2 \\ 0.01 & 0.01 & 0.1 \end{bmatrix}, \quad H_1 = \begin{bmatrix} 0.001 & 1 & 0 \\ 1 & 0.2 & 0 \\ 0.001 & 0.003 & 1 \end{bmatrix},$$

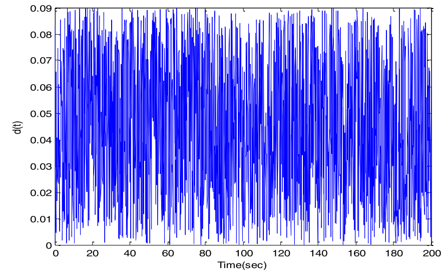

FIGURE 1. Disturbance.

$$H_2 = \begin{bmatrix} 0.001 & 1 & 0.001 \\ 1 & 0.2 & 0.003 \\ 0 & 0 & 1 \end{bmatrix}, \quad J_1 = \begin{bmatrix} 0.03 & 0.03 & 0.03 \\ 0 & 0 & 0 \\ 0.23 & 0.23 & 0.23 \end{bmatrix},$$

$$J_2 = \begin{bmatrix} 0.06 & 0.06 & 0.06 \\ 0 & 0 & 0 \\ 0.03 & 0.03 & 0.03 \end{bmatrix}, \quad D_1 = D_2 = \begin{bmatrix} 0.1 & 0 & 0 \\ 0 & 0.1 & -1 \end{bmatrix}.$$

Setting the prerequisite variable of Type-II fuzzy system as x_2, the membership functions are:

$$\begin{cases} \mu_{\xi_{i1},low}(x_2 = 0.2) = \exp[-((x_2 + 0.5)/0.44)^2] \\ \mu_{\xi_{i1},up}(x_2 = 0.2) = \exp[-((x_2 + 0.5)/0.36)^2] \\ \mu_{\xi_{i1},low}(x_2 = 0.8) = 1 - \exp[-((x_2 + 0.5)/0.36)^2] \\ \mu_{\xi_{i1},up}(x_2 = 0.8) = 1 - \exp[-((x_2 + 0.5)/0.44)^2] \end{cases}$$

Define two fuzzy rules: Rule 1: IF x_2 is approximately 0.2, THEN: $i = 1$, $\{A_1\ B_1\ H_1\ J_1\ D_1\}$; Rule 2: IF x_2 is approximately 0.8, THEN: $i = 2$, $\{A_2\ B_2\ H_2\ J_2\ D_2\}$.

According to the definition of the actuator time-varying step fault, the value of $F_{tvs}(t)$ is

$$F_{tvs}(t) = [F_{1tvs}(t)\ F_{2tvs}(t)\ F_{3tvs}(t)]^T \tag{83}$$

$$F_{1tvs}(t) = F_{2tvs}(t) = F_{3tvs}(t) \tag{84}$$

$$F_{1tvs}(t) = \begin{cases} F_{1\sigma}(t), & t \in (t_{\sigma 1}, t_{\sigma 2}] \\ 0, & otherwise \end{cases} \tag{85}$$

Considering $\sigma_0 = 2$, and set the fault window intervals, the fault assignment is given as

$$F_{1tvs}(t) = \begin{cases} F_{11}(t), & t \in (20s, 80s] \\ F_{12}(t), & t \in (100s, 160s] \\ 0, & otherwise \end{cases}$$

$$F_{11}(t) = \begin{cases} F_{11,inc}(t), & t \in (20s, 40s] \\ F_{11,non-inc}(t), & t \in (40s, 80s] \end{cases}$$

$$F_{12}(t) = \begin{cases} F_{12,inc}(t), & t \in (100s, 120s] \\ F_{12,non-inc}(t), & t \in (120s, 160s] \end{cases}$$

$$\begin{cases} F_{11,inc}(t) = F_{12,inc}(t) = 0.2, \\ \quad t \in (20s, 40s],\ (100s, 120s] \\ F_{11,non-inc}(t) = F_{12,non-inc}(t) = 1.2, \\ \quad t \in (40s, 60s],\ (120s, 140s] \\ F_{11,non-inc}(t) = F_{12,non-inc}(t) = 1, \\ \quad t \in (60s, 80s],\ (140s, 160s] \end{cases}$$

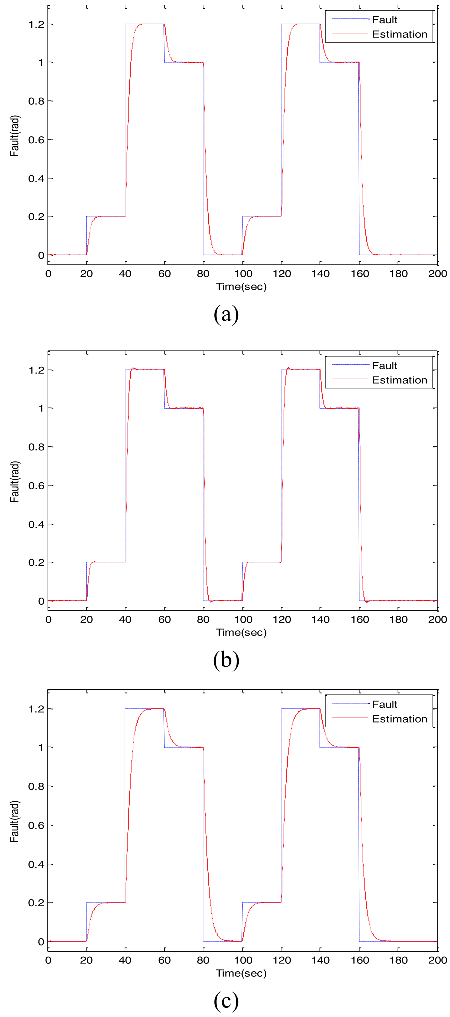

FIGURE 2. Estimation for actuator faults. (a) $F_{1tvs}(t)$. (b) $F_{2tvs}(t)$. (c) $F_{3tvs}(t)$.

TABLE 3. Tracking performance indicators for rudder faults.

	$F_{1tvs}(t)$	$F_{2tvs}(t)$	$F_{3tvs}(t)$
$E_{T1,fd}$	0.0014	0.0083	0.0054
$E_{T2,fd}$	0.0057	0.0219	0.0133
$E_{T3,fd}$	0.0052	0.0171	0.0098
$E_{T4,fd}$	0.0011	0.0012	0.0011
$T_{T1,fd}$	5.7362s	2.8235s	3.1287s
$T_{T2,fd}$	6.3948s	2.9023s	4.9007s
$T_{T3,fd}$	5.4459s	2.8874s	3.1152s
$T_{T4,fd}$	6.2811s	2.8696s	4.8916s

TABLE 4. Tracking performance indicators for output pdfs.

	ρ_1	ρ_2	ρ_3
$E_{T1,ftc}$	0.0014	0.0083	0.0054
$E_{T2,ftc}$	0.0027	0.0109	0.0083
$E_{T3,ftc}$	0.0022	0.0091	0.0078
$E_{T4,ftc}$	0.0011	0.0012	0.0011
$T_{T1,ftc}$	5.84s	3.01s	3.33s
$T_{T2,ftc}$	6.70s	3.03s	5.18s
$T_{T3,ftc}$	5.84s	3.04s	3.33s
$T_{T4,ftc}$	6.66s	2.99s	5.15s

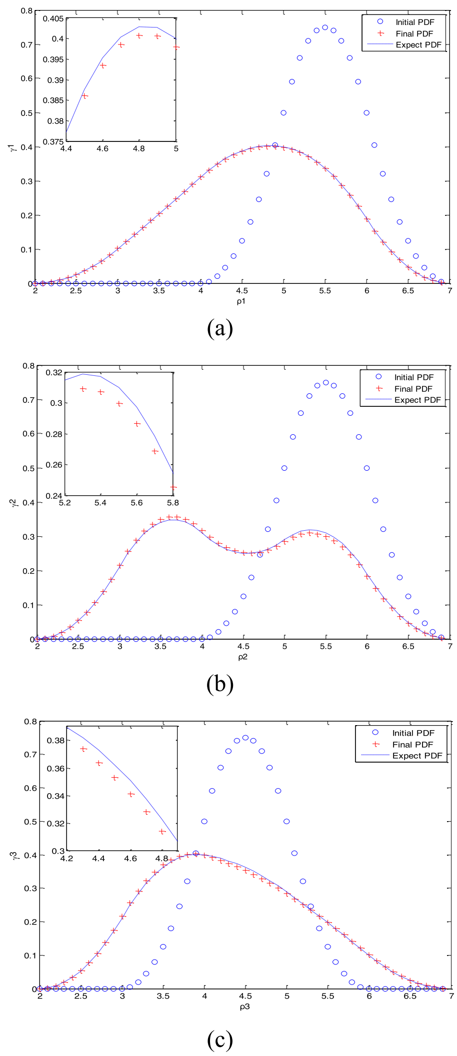

FIGURE 3. Compensation for output PDFs. (a) γ_1. (b) γ_2. (c) γ_3.

The deviation disturbance $d(t)$ satisfies: $d_g = 0.045+$ randn (0.015, 2000), acquisition time: $0.1s$. Fig. 1 shows the curve.

In Theorem 1, setting $C_{11} = C_{12} = [0.10.10.1]$, $C_{21} = C_{22} = 0.1$ and $\lambda_1 = \lambda_2 = 0.2$, we can obtain: $P = [0.0587 - 0.04750; -0.04750.24190; 00 - 0.4375]$, $L_1 = [2.3495; 2.5783; -0.0664]$, $L_2 = [3.1255; 2.9289; -0.0890]$. The fuzzy-prey fusion adaptive parameters are: $\Gamma_{111} = 0.0043$, $\Gamma_{121} = 0.0055$, $\Gamma_{211} = 2.0135$, $\Gamma_{221} = 2.0148$, $\Gamma_{112} = 0.0043$, $\Gamma_{122} = 0.0033$, $\Gamma_{212} = 2.0135$, $\Gamma_{222} = 2.0111$. The system state and its estimated initial values are $[0.1\ 0.1\ 0.1]^T$. Setting the desired weight vector $V_{expe} = [0.20.42]$, the switching threshold $\kappa = 0.003$, $\lambda_3 = 0.2$, $C_{14} = C_{24} = [0.10.10.10.10.1]$. Fig. 2 shows the fault estimation results. The elements of the parameter matrices are not equal, and the tracking curves of three angles are also different. The time-varying step fault is divided into four time periods:

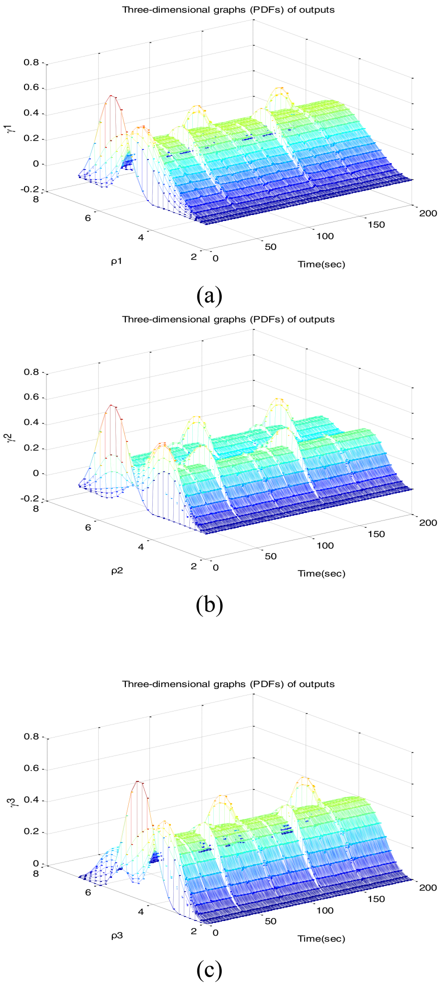

FIGURE 4. **Three-dimensional attitude angle PDFs. (a) γ_1. (b) γ_2. (c) γ_3.**

incipient amplitude time period T1 (20 s-40 s, 100 s-120 s), large amplitude time periods T2 (40 s-60 s, 120 s-140 s) and T3 (60 s-80 s, 140 s-160 s), intermediate fault-free period T4 (80 s-100 s). Table 3 summarizes the tracking performance indicators of the three actuator faults in four periods, including static error $E_{\mathrm{T1},fd}$, $E_{\mathrm{T2},fd}$, $E_{\mathrm{T3},fd}$ and $E_{\mathrm{T4},fd}$ and response time $T_{\mathrm{T1},fd}$, $T_{\mathrm{T2},fd}$, $T_{\mathrm{T3},fd}$ and $T_{\mathrm{T4},fd}$.

Fig. 2 shows that the estimation algorithm can effectively track the three elements of the actuator fault vector.

According to Theorem 2, the gain matrices can be determined including the parameters that are freely adaptable and satisfy the calculation results: Ω_{11}, Ω_{12}, Ω_{21}, Ω_{22}, Γ_{i3} and Γ_{i4}. The dimension choice of Γ_{i3} and Γ_{i4} can solve dimensional matching problems. The gain matrices are solved by LMI and continuous test as follows where semicolon represents a new matrix row: $\Omega_{11} = [-2.1678 - 1.1623 - 1.7077 - 3.2486 - 3.2489; -2.1678 - 1.1623 - 1.7077 - 3.2486 - 3.2489; -2.1678 - 1.1623 - 1.7077 - 3.2486 - 3.2489]$, $\Omega_{12} = [1.6835 - 3.9531 - 0.2425 - 2.1978 - 2.0785; 1.6835 - 3.9531 - 0.2425 - 2.1978 - 2.0785; 1.6835 - 3.9531 - 0.2425 - 2.1978 - 2.0785]$, $\Omega_{21} = [-2.1700 - 3.4030 - 4.7649 - 7.0740 - 7.0742; -2.1700 - 3.4030 - 4.7649 - 7.0740 - 7.0742; -2.1700 - 3.4030 - 4.7649 - 7.0740 - 7.0742]$, $\Omega_{22} = [1.1239 - 3.7655 - 0.3124 - 2.2248 - 2.1859; 1.1239 - 3.7655 - 0.3124 - 2.2248 - 2.1859; 1.1239 - 3.7655 - 0.3124 - 2.2248 - 2.1859]$, $\Gamma_{i3} = 1$, $\Gamma_{i4} = [-0.8301 - 0.2044 - 1.1797 - 0.5332 - 0.5332]$. Table 4 summarizes the tracking performance indicators of three output PDFs in four periods, including static error $E_{\mathrm{T1},ftc}$, $E_{\mathrm{T2},ftc}$, $E_{\mathrm{T3},ftc}$ and $E_{\mathrm{T4},ftc}$ and response time $T_{\mathrm{T1},ftc}$, $T_{\mathrm{T2},ftc}$, $T_{\mathrm{T3},ftc}$ and $T_{\mathrm{T4},ftc}$. Static error: the maximum deviation of the actual three-dimensional PDF surface from the ideal three-dimensional PDF surface after stabilization, response time: the corresponding time of the earliest time profile function that any deviation between actual and ideal PDF values is in 3%.

Table 4 shows that the performance index of time period T2 is the worst but still fast and accurate and remains within the engineering allowable range. Fig. 3 shows the results of FTC in T2.

Figs. 3(a)-(c) show the tracking results of the three output PDFs at $t = 55$ s. Since the shape of the second fault window is same as that of the first one, only the first one is shown. In order to fully display the tracking results of PDFs, Figs. 4(a)-(c) show the three-dimensional tracking results of FTC. It is obvious that, regardless of whether there is a fault, the output PDFs can accurately track the given PDFs at any time.

VI. CONCLUSION

This paper considers systems with multiple stochastic outputs, singularity and disturbance to establish non-Gaussian stochastic systems. An active-passive hybrid FTC scheme is designed for the compound faults with actuator and sensor initial faults. Using the improved adaptive PDC FTC strategies to control the systems is a novel and practical strategy. Both the estimation observer and FTC systems are proven to be robust and stable. In the actuator fault estimation and compound FTC algorithms, the adaptive learning rates fuse fault amplitude and fuzzy premise variable information, ensure reliable and flexible control. Simultaneously the passive compensation factors effectively shield the sensor initial fault. The effectiveness of fault estimation and FTC are verified by the simulation. Finally, the output PDFs match the expected PDFs. This technique can address the issues with control of multiple stochastic output systems such as stochastic attitude hypersonic flight vehicles and aeroengine plume.

ACKNOWLEDGMENT

The authors would like to thank Kaiyu Hu's mentor Professor Fuyang Chen for his guidance.

REFERENCES

[1] C. R. Chen, T. He, D. Y. Wu, Q. Pan, H. Wang, and X. F. Liu, "Advances in prognostics and system health management," *IEEE Access*, vol. 6, pp. 78483–78492, 2018.

[2] R. Yu, J.-P. Cai, and B.-R. Wang, "Adaptive failure compensation of actuators in controlling servo system driven by twin motors," *IEEE Access*, vol. 6, pp. 63223–63231, 2018.

[3] Y. Lin, J. Du, G. Zhu, and J. Li, "Output feedback thruster fault-tolerant control for dynamic positioning of vessels under input saturation," *IEEE Access*, vol. 6, pp. 76271–76281, 2018.
[4] S. K. Kommuri, S. B. Lee, and K. C. Veluvolu, "Robust sensors-fault-tolerance with sliding mode estimation and control for PMSM drives," *IEEE/ASME Trans. Mechatronics*, vol. 23, no. 1, pp. 17–28, Feb. 2018.
[5] A. Kodali, K. Pattipati, and S. Singh, "Coupled factorial hidden Markov models (CFHMM) for diagnosing multiple and coupled faults," *IEEE Trans. Syst., Man, Cybern. Syst.*, vol. 43, no. 3, pp. 522–534, May 2013.
[6] Z. G. Yi, N. Pan, and Y. Guo, "Mechanical compound faults extraction based on improved frequency domain blind deconvolution algorithm," *Mech. Syst. Signal Process.*, vol. 113, pp. 180–188, Dec. 2018.
[7] Q. K. Shen, B. Jiang, and P. Shi, "Adaptive fault diagnosis for T–S fuzzy systems with sensor faults and system performance analysis," *IEEE Trans. Fuzzy Syst.*, vol. 22, no. 2, pp. 274–285, Apr. 2014.
[8] V. Reppa, M. M. Polycarpou, and C. G. Panayiotou, "Decentralized isolation of multiple sensor faults in large-scale interconnected nonlinear systems," *IEEE Trans. Autom. Control*, vol. 60, no. 6, pp. 1582–1596, Jun. 2015.
[9] S. T. Wan, X. Zhang, and L. J. Dou, "Compound fault diagnosis of bearings using improved fast spectral kurtosis with VMD," *J. Mech. Sci. Technol.*, vol. 32, no. 11, pp. 5189–5199, Nov. 2018.
[10] W. Fan, Q. Zhou, J. Li, and Z. K. Zhu, "A wavelet-based statistical approach for monitoring and diagnosis of compound faults with application to rolling bearings," *IEEE Trans. Autom. Sci. Eng.*, vol. 15, no. 4, pp. 1563–1572, Oct. 2015.
[11] Q. K. Shen, B. Jiang, and V. Cocquempot, "Fault-tolerant control for T–S fuzzy systems with application to near-space hypersonic vehicle with actuator faults," *IEEE Trans. Fuzzy Syst.*, vol. 20, no. 4, pp. 652–665, Aug. 2012.
[12] J.-X. Zhang and G.-H Yang, "Prescribed performance fault-tolerant control of uncertain nonlinear systems with unknown control directions," *IEEE Trans. Autom. Control*, vol. 62, no. 12, pp. 6529–6535, Dec. 2017.
[13] Q. Hu, X. Shao, and L. Guo, "Adaptive fault-tolerant attitude tracking control of spacecraft with prescribed performance," *IEEE/ASME Trans. Mechatronics*, vol. 23, no. 1, pp. 331–341, Feb. 2018.
[14] G. Li, T. Li, and Q. Zhao, "Fault tolerant shape control for particulate process systems under simultaneous actuator and sensor faults," *IET Control Theory Appl.*, vol. 11, no. 15, pp. 2448–2457, Oct. 2017.
[15] X. Li, D. Lu, G. Zeng, J. Liu, and W. Zhang, "Integrated fault estimation and non-fragile fault-tolerant control design for uncertain takagi–sugeno fuzzy systems with actuator fault and sensor fault," *IET Control Theory Appl.*, vol. 11, no. 10, pp. 1542–1553, Jun. 2017.
[16] S. Yin, H. Yan, and O. Kaynak, "Sliding mode observer-based FTC for markovian jump systems with actuator and sensor faults," *IEEE Trans. Autom. Control*, vol. 62, no. 7, pp. 3551–3558, Jul. 2017.
[17] T. Sun, D. Liang, and Y. M. Song, "Singular-perturbation-based nonlinear hybrid control of redundant parallel robot," *IEEE Trans. Ind. Electron.*, vol. 65, no. 4, pp. 3326–3336, Apr. 2018.
[18] X. Zhang, H. Su, and R. Lu, "Second-order integral sliding mode control for uncertain systems with control input time delay based on singular perturbation approach," *IEEE Trans. Autom. Control*, vol. 60, no. 11, pp. 3095–3100, Nov. 2015.
[19] L. Liu, S. Dong, Y. J. Wang, and L. L. Ou, "Clearance of flight control law based on structural singular value theory," *IEEE Trans. Aerosp. Electron. Syst.*, vol. 51, no. 3, pp. 2138–2147, Jul. 2015.
[20] S. Wang and J. Huang, "Cooperative output regulation of singular multi-agent systems under switching network by standard reduction," *IEEE Trans. Circuits Syst. I, Reg. Papers*, vol. 65, no. 4, pp. 1377–1385, Apr. 2018.
[21] C. Mu, Q. Zong, B. L. Tian, and W. Xu, "Continuous sliding mode controller with disturbance observer for hypersonic vehicles," *IEEE/CAA J. Autom. Sinica*, vol. 2, no. 1, pp. 45–55, Jan. 2015.
[22] Q. Hu, X. D. Shao, and W.-H. Chen, "Robust fault-tolerant tracking control for spacecraft proximity operations using time-varying sliding mode," *IEEE Trans. Aerosp. Electron. Syst.*, vol. 54, no. 1, pp. 2–17, Feb. 2018.
[23] C. Sendi and M. A. Ayoubi, "Robust fuzzy tracking control of flexible spacecraft via a T–S fuzzy model," *IEEE Trans. Aerosp. Electron. Syst.*, vol. 54, no. 1, pp. 170–179, Feb. 2018.
[24] Y. Kang, L. Zhao, and L. Yao, "Fault diagnosis and model predictive fault tolerant control for stochastic distribution collaborative systems," *Int. J. Model., Identificat. Control*, vol. 30, no. 1, pp. 30–37, Jul. 2018.
[25] H. Wang, H. Baki, and P. Kabore, "Control of bounded dynamic stochastic distributions using square root models: An applicability study in papermaking systems," *Trans. Inst. Meas. Control*, vol. 23, no. 1, pp. 51–68, Mar. 2001.
[26] L. N. Yao and C. H. Lei, "Fault diagnosis and sliding mode fault tolerant control for non-Gaussian stochastic distribution control systems using T–S fuzzy model," *Asian J. Control*, vol. 19, no. 2, pp. 636–646, Mar. 2017.
[27] L. Yao, C. Lei, Y. Guan, and H. Wang, "Minimum entropy fault-tolerant control for non-Gaussian singular stochastic distribution systems," *IET Control Theory Appl.*, vol. 10, no. 10, pp. 1104–1201, Jun. 2016.
[28] Y. C. Sun and L. N. Yao, "Robust fault diagnosis and fault-tolerant control for non-Gaussian uncertain stochastic distribution control systems," *Int. J. Robust Nonlinear Control*, vol. 27, no. 10, pp. 1709–1725, Jul. 2017.
[29] T. Li, G. Li, and Q. Zhao, "Adaptive fault-tolerant stochastic shape control with application to particle distribution control," *IEEE Trans. Syst., Man, Cybern. Syst.*, vol. 45, no. 12, pp. 1592–1604, Dec. 2015.

KAIYU HU received the B.E. degree in automation from Jilin University, Changchun, China, in 2012, and the M.S. degree in astrophysics from the University of Chinese Academy of Sciences, Beijing, China, in 2015. He is currently pursuing the Ph.D. degree with the Nanjing University of Aerobautics and Astronautics, Nanjing, China.

His research interests include adaptive control, non-Gaussian systems, and fault-tolerant control.

CHANGYUN WEN received the B.Eng. degree from Xi'an Jiaotong University, in 1983, and the Ph.D. degree from The University of Newcastle, Australia, in 1990.

From 1989 to 1991, he was a Research Associate and then a Postdoctoral Fellow with The University of Adelaide, Australia. Subsequently, he joined the School of Electrical and Electronic Engineering, Nanyang Technological University (NTU), as a Lecturer, where he was promoted to Full Professor through the first Promotion and Tenure Review Exercise, in 2008. His main research activities are in the areas of adaptive control, intelligent power management system for more electric aircraft, modelling and control of active chilled beam for HVAC systems, switching and impulsive systems, and model based online learning.

AILI YUSUP received the B.E. degree from Peking University.

He is currently a Researcher and the Chief Engineer of the Xinjiang Astronomical Observatory of National Astronomical Observatories, Chinese Academy of Sciences. He attends and manages a lot of important projects, such as the China Lunar Exploration, Mars Exploration, 973, and NSFC. He is currently hosting the project of upgrading for 25m antenna. He has also visited many observatories in USA and Australia and finished many special beacons independently. His current interests include TT & C systems, software of antenna control systems, and satellite communications.